ETEAPOT PTR Benchmark-II:
Transfer Matrices and Twiss Functions

J. D. Talman and R. M. Talman

August 26, 2923

Abstract

In this chapter ETEAPOT is used to obtain transfer matrices between arbitrary lattice positions, and, from them, Twiss functions as functions of longitudinal coordinate s. Three new PTR sxf files now replace three benchmark lattices processed in the November 6, 2019, "ETEAPOT EDM Benchmark I: Updated Results for Proton EDM Benchmark Lattices". The lattices have field indices $m = 0.29447$, $m = 0.32349$, and $m = 0.39447$, which represent a much reduced range of electrode shapes than the earlier report (as well as corresponding to the PTR "predominantly electric lattice" rather than the "proton EDM lattice"). Once-around transfer matrices are obtained and used to determine beta functions at the origin as well as transverse tunes. In Benchmark I, tunes have been obtained using multiturn tracking (thereby avoiding aliasing ambiguity) but general transfer matrices and beta functions were not obtained and the issue of aliasing ambiguities affecting the determination of integer tune values was only mentioned. This report addresses these deficiencies. Results are compared to values obtained from a linearized MAPLE transfer matrix BSM formalism. In all cases the lumped quadrupole strengths have been reduced to a common (small enough to be relatively unimportant) value for which the vertical betatron motion is conservatively stable.

1 Determination of Twiss Functions From Transfer Matrices

Table 1 contains PTR position and length parameters as well as tune values obtained in the PTR-Benchmark-I report. The "same" three lattices that were processed in the PTR Benchmark-I report are processed in this PTR-Benchmark-II report. The reason for "same" to be in quotation marks is that, though the geometrry is identical, though very weak, the quadrupole strengths are not the same in Benchmark-I and Benchmark-II. This complication is brought about by the newly introduced concept of "compromise quadrupoles" which need to be employed for "predominantly electric bending" for which some quads are electric, some magnetic.

2 Analysis of the Once-Around Transfer Matrix at the Origin

In this section x and y and ct subscripts will be suppressed, and only transverse evolution is to be discussed. The most general transfer matrix is a six-by-six matrix $\mathbf{M}(s_i, s_j)$, which propagates a phase space vector $\mathbf{x}(s_i)$ at s_i, to its value $\mathbf{x}(s_j)$ at s_j;

$$\mathbf{x}(s_j) = \mathbf{M}(s_i, s_j)\, \mathbf{x}(s_i). \tag{1}$$

ETEAPOT starts by assigning coordinates at the origin, $s_0 = 0$, to the particles in a standard bunch (as described earlier), and then evolves the standard bunch and records the coordinates $\mathbf{x}(s_i)$ at all points s_i. From these results the transfer matrices $\mathbf{M}(0, s_i)$ can be calculated (also as described earlier). By definition

$$\mathbf{M}(0,0) = \mathbf{I}, \tag{2}$$

where $\mathbf{I}$ is the 6×6 identity matrix.

To extract Twiss lattice functions one needs periodic, "once-around" transfer matrices, distinguished by overhead tildes, and defined by

$$\widetilde{\mathbf{M}}(s_i) \equiv \mathbf{M}(s_i, s_i + \mathcal{C}_0) = \mathbf{M}(0, s_i)\, \mathbf{M}(s_i, \mathcal{C}_0). \tag{3}$$

where $\mathcal{C}_0$ is the circumference of the design orbit; the final step has been taken because knowledge of $s_i + \mathcal{C}_0$ requires tracking for more than one complete turn, but we are assuming that tracking has been done only for exactly one complete turn. Propagation from $s = \mathcal{C}_0$ to $\mathcal{C}_0 + s_i$ is the same as propagation from $s = 0$ to s_i. The Twiss parameterization of (one partitioned diagonal 2×2 block of) such a once-around, symplectic transfer matrix is

$$\widetilde{\mathbf{M}}(s_i) = \begin{pmatrix} \cos\mu + \alpha\sin\mu & \beta\sin\mu \\ -\frac{1+\alpha^2}{\beta}\sin\mu & \cos\mu - \alpha\sin\mu \end{pmatrix}. \tag{4}$$

Extraction of the α_0 and β_0, the Twiss parameters at the origin, can start from

$$\cos\mu = \frac{1}{2}\left(\widetilde{\mathbf{M}}_{11}(0) + \widetilde{\mathbf{M}}_{22}(0)\right), \tag{5}$$

which fixes $\cos\mu$. Because of sign ambiguity, this determines only $|\sin\mu|$. One also has the relations

$$\beta_0 = \left| \frac{\widetilde{\mathbf{M}}_{12}(0)}{\sin\mu} \right|. \tag{6}$$

and

$$\alpha_0 = \frac{1}{2\sin\mu}\left(\widetilde{\mathbf{M}}_{11}(0) - \widetilde{\mathbf{M}}_{22}(0)\right). \tag{7}$$

With β being positive by convention, from the 1,2 element, $\mathrm{sign}(\sin\mu)$ can be seen to be the same as $\mathrm{sign}(\widetilde{\mathbf{M}}_{12})$. With $\cos\mu$ known, this fixes $\sin\mu$. Together, these relations fix $\sin\mu$, $\cos\mu$, α_0, and β_0.

Conventionally one also introduces a third Twiss parameter

$$\gamma_0 = \frac{1 + \alpha_0^2}{\beta_0}, \tag{8}$$

which can be obtained once β_0 and α_0 have been determined.

Because of the multiple-valued nature of inverse trig functions, these relations do not determine a unique value for μ. They do, however, determine the quadrant in phase space in which the angle μ resides. For $\mathrm{sign}(\sin\mu) > 0$ the angle μ resides in the first or second quadrant, in which case the fractional tune is less than $1/2$; otherwise the fractional tune is greater than $1/2$. For $\mathrm{sign}(\cos\mu) > 0$ the angle μ resides in the first or fourth quadrant, in which case the fractional tune is below $1/4$ or above $3/4$. These considerations fix the fractional parts of the tunes.

An "aliasing" or "integer-tune" ambiguity remains, however, which cannot, even in principle, be obtained from the once-around matrix. Only if both transverse tunes are less than 1 (which is hardly ever the case) would the tunes be equal to the fractional tunes that have been determined. In general, to obtain the integer tunes, it is necessary to analyse the turn by turn data at sufficiently closely-space intermediate points in the lattice, or for multiple turns. (See examples in the previous chapter.)

3 Evolving the Twiss Functions Around the Ring

To find the Twiss parameters at an arbitrary location s_i in the ring requires the once-around transfer matrix $\widetilde{\mathbf{M}}(s_i)$. This can obtained most compactly by multiplying the equation

$$\mathbf{M}(0, s_j) = \mathbf{M}(s_i, s_j)\,\mathbf{M}(0, s_i) \tag{9}$$

on the right by $\mathbf{M}^{-1}(0, s_i)$ to produce

$$\mathbf{M}(s_i, s_j) = \mathbf{M}(0, s_j)\,\mathbf{M}^{-1}(0, s_i). \tag{10}$$

Substituting this with $s_j = \mathcal{C}_0$ into Eq. (3) produces

$$\widetilde{\mathbf{M}}(s_i) = \mathbf{M}(0, s_i)\,\widetilde{\mathbf{M}}(0)\,\mathbf{M}^{-1}(0, s_i). \tag{11}$$

Having obtained $\widetilde{\mathbf{M}}(s_i)$, the procedure described in the previous subsection can then be used to obtain $\alpha(s_i)$ and $\beta(s_i)$. But the integer tune ambiguity can, again, not be resolved. To resolve this ambiguity both x and y phases have to be tracked continuously through the lattice, requiring that they advance continuously and monotonically. (Later, at least in principle, the same ambiguity will have to be faced for longitudinal motion. But the integer longitudinal tune is almost always zero, so the problem is usually absent in the longitudinal case.)

ETEAPOT requires the lattice description to be in the form of an `.sxf` file. To be "legal" the granularity of such a file has to be fine enough that no phase can advance by more than a quarter integer through any element in the file. Before working out the α and β function evolution, ETEAPOT first works out the total phase advances from the origin to every node specified by the `.sxf` file (or, if some elements are sliced more finely, by every node after slicing).

There is an alternative way of finding the betatron phase advances. It starts with a Twiss parameterization of $\mathbf{M}(0, s)$ from the origin to an arbitrary position s in the lattice;

$$\mathbf{M}(0, s) = \begin{pmatrix} \sqrt{\frac{\beta(s)}{\beta_0}}\Big(\cos\psi(s) + \alpha_0\sin\psi(s)\Big) & \sqrt{\beta_0\beta(s)}\,\sin\psi(s) \\ \cdot & \sqrt{\frac{\beta_0}{\beta(s)}}\Big(\cos\psi(s) - \alpha(s)\sin\psi(s)\Big) \end{pmatrix}. \tag{12}$$

The 2,1 element is quite complicated; it is not shown here since it will not be needed for the following analysis. Dividing the 1,1 element by the 1,2 element produces

$$\frac{\mathbf{M}_{1,1}(0, s)}{\mathbf{M}_{1,2}(0, s)} = \frac{\sqrt{\frac{\beta(s)}{\beta_0}}\Big(\cos\psi(s) + \alpha_0\sin\psi(s)\Big)}{\sqrt{\beta_0\beta(s)}\,\sin\psi(s)} = \frac{\cot\psi(s) + \alpha_0}{\beta_0}. \tag{13}$$

Rearranging this equation produces

$$\psi(s) = \tan^{-1}\frac{\mathbf{M}_{1,2}(0, s)}{\beta_0\mathbf{M}_{1,1}(0, s) - \alpha_0\mathbf{M}_{1,2}(0, s)}. \tag{14}$$

Like all inverse trigonometric formulas, this equation has multiple solutions. But, with the `.sxf` granularity being required to be fine enough, one can (in principle) sequentially obtain unique phases. With $\psi(s)$ starting from $\psi(0) = 0$, as s increases from s_i to s_{i+1} there is a unique solution of Eq. (14), $\psi(s_i) \geq \psi(s_{i-1})$ such that the function $\psi(s)$ increases monotonically, as required. Because the interval from $s_{i=1}$ to s_i is non-zero, ψ will, superficially, advance discontinuously; the correct solution is the least discontinuous. The same calculation has to be done for both the x and y betatron sectors. Unfortunately, even though, theoretically, the phase advances monotonically, numerical errors can cause Eq. (14) to give local phase decrease. This can cause Eq. (14) to give occasionally erratic results.

4 ETEAPOT and MAPLE results for barely stable PTR ring

This section compares beta functions for three PTR lattice settings which are at least close to being stable in both transverse planes, with all quadrupoles very weak, just strong enough for near stability, as calculated by UAL:ETEAPOT and MAPLE. Tracked for hundreds of turns these beta functions would eventually diverge. As mentioned previously, due partly to the "compromise quadrupoles" in the sxd files, the quadrupole strengths, though weak, are not exactly the same for UAL:ETEAPOT and MAPLE.

Loosely speaking, processed in this way, this ring is four identical 90 degree electric spectrometers arranged in a circle, not yet adjusted for long term stability.

Symmetry excludes the exact superposition of thin magnetic and electric quadrupoles—if the electrodes have the same profiile as the iron poles then the the electric and magnetic quads would relyively skew. Thin "compromise quadrupoles" are actually quadrupole BEB triplets with B and E adjusted such that, in thin lens approximation, the triplet is equivalent to a thick superimposed EM quadrupole. Of course the final effective quadrupole can neither very strong nor very short.

For the proposed predominantly electric ring being proposed this constraint is not very serious. It will, however, limit the ability to produce ultra small beta functions at the IPs.
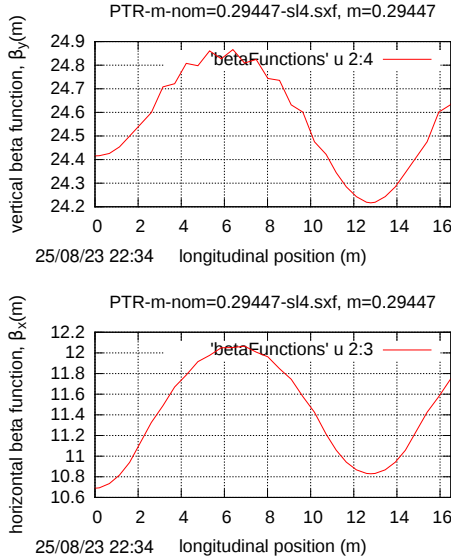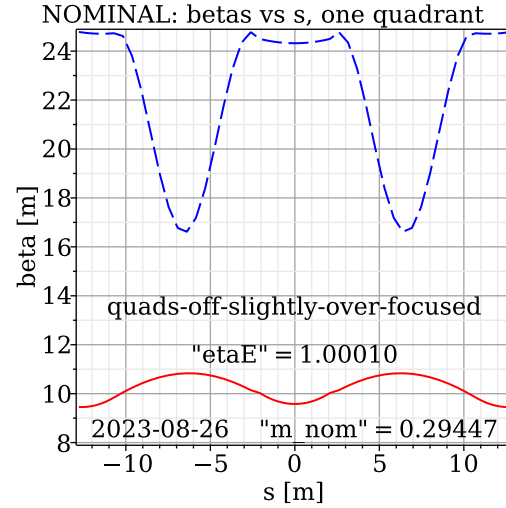
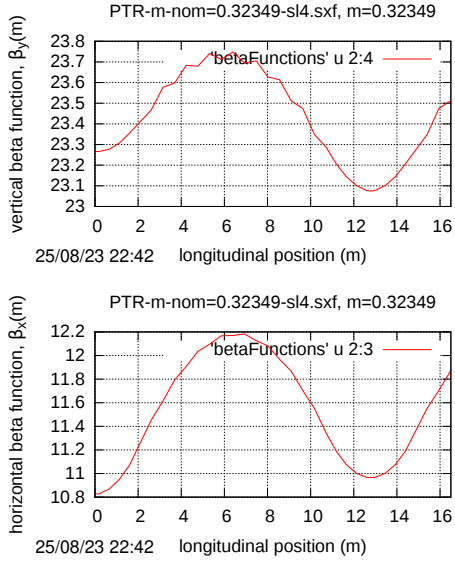Figure 1: UAL:ETEAPOT results
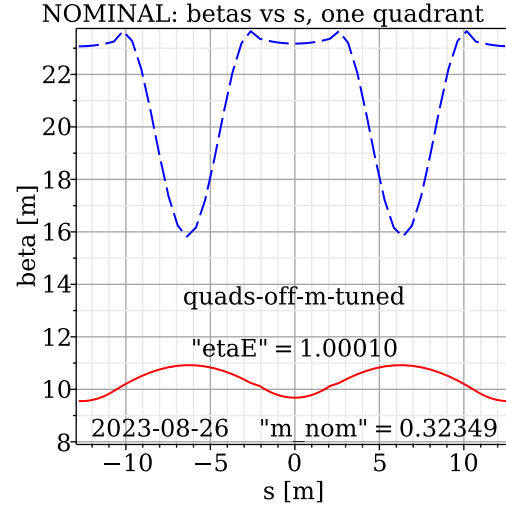
Figure 2: MAPLE results.
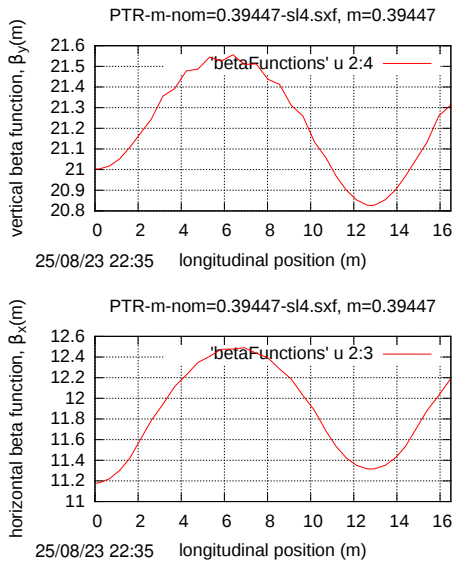
Figure 3: UAL:ETEAPOT results

Figure 4: MAPLE results.

Figure 5: UAL:ETEAPOT results
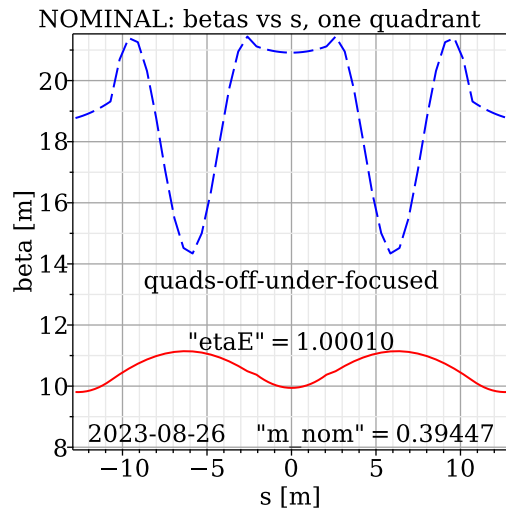

Figure 6: MAPLE results.

5

4.1 Parameters of PTR Benchmark Lattices

	variable name	unit	PTR_m=0.29447	m=0.32349	m=0.39447
cells/arc	NCellPerOctant		1	1	1
bend radius	r0	m	11.0	11.0	11.0
long drift length	llsnom	m	4.14214	4.14214	4.14214
half bend of cell	lh	r	$2\pi/16$	$2\pi/16$	$2\pi/16$
half bend length	leh	m	$2\pi r0/16$	$2\pi r0/16$	$2\pi r0/16$
circumference	circum	m	102.252	102.252	102.252
inverse focal length	delq	1/m	-0.009091	-0.009091	-0.009091
field index	m		0.29447	0.32349	0.39447
UAL horz beta	betax	m	≈ 11.4	≈ 11.6	≈ 11.9
UAL vert beta	betay	m	≈ 24.6	≈ 23.4	≈ 21.2
MAPLE horz beta	betax	m	≈ 10	≈ 10.2	≈ 10.5
MAPLE vert beta	betay	m	≈ 22	≈ 21	≈ 18.5
horizontal tune	Qx				
vertical tune	Qy				
BM-I, horz. tune	Qx		1.42	1.40	1.355
BM-I, vert. tune	Qy		0.655	0.655	0.76

Table 1: Parameters of PTR benchmark lattices, including tunes determined in PTR-benchmark-I investigation for the same three electrode shape parameters, but slightly different (though weak) quadrupole strength values. The two bottom rows are copied from the PTR-BM-I report. The (approximate) beta function values are read from the plots above. They are recorded as approximate since the rings are only marginally stable.

References

[1] J.D. Talman and R.M. Talman, *UAL/ETEAPOT Results (Augmented) for Proton EDM Benchmark Lattices,* BNL internal report, April 29, 2012

[2] N. Malitsky, J. Talman, and R. Talman, *Appendix UALcode: Development of the UAL/ETEAPOT Code for the Proton EDM Experiment,* UAL/ETEAPOT documentation (frequently revised), August, 2012

[3] Storage Ring EDM Collaboration, *A Proposal to Measure the Proton Electric Dipole Moment with 10^{-29} e-cm Sensitivity,* especially Appendix 1. October, 2011

[4] C. Møller, *The Theory of Relativity,* Clarendon Press, Oxford, 1952,

[5] G. Muñoz and I. Pavic, *A Hamilton-like vector for the special-relativistic Coulomb problem,* Eur. J. Phys. **27**, 1007-1018, 2006

[6] R. Talman, *Geometric Mechanics,* John Wiley and Sons, 2000

[7] J. Aguirregabiria et al., Archiv:physics/0407049v1 [physics.ed-ph] 2004,

[8] U. Torkelsson, Eur. J. Phys., **19**, 459, 1998,

[9] T. Boyer, Am. J. Phys. **72** (8) 992, 2004